nature biotechnology

Second-harmonic imaging microscopy for visualizing biomolecular arrays in cells, tissues and organisms

Paul J Campagnola & Leslie M Loew

Although the nonlinear optical effect known as second-harmonic generation (SHG) has been recognized since the earliest days of laser physics and was demonstrated through a microscope over 25 years ago, only in the past few years has it begun to emerge as a viable microscope imaging contrast mechanism for visualization of cell and tissue structure and function. Only small modifications are required to equip a standard laser-scanning two-photon microscope for second-harmonic imaging microscopy (SHIM). Recent studies of the three-dimensional *in vivo* structures of well-ordered protein assemblies, such as collagen, microtubules and muscle myosin, are beginning to establish SHIM as a nondestructive imaging modality that holds promise for both basic research and clinical pathology. Thus far the best signals have been obtained in a transmitted light geometry that precludes *in vivo* measurements on large living animals. This drawback may be addressed through improvements in the collection of SHG signals via an epi-illumination microscope configuration. In addition, SHG signals from certain membrane-bound dyes have been shown to be highly sensitive to membrane potential. Although this indicates that SHIM may become a valuable tool for probing cell physiology, the small signal size would limit the number of photons that could be collected during the course of a fast action potential. Better dyes and optimized microscope optics could ultimately lead to the imaging of neuronal electrical activity with SHIM.

SHIM is based on the familiar nonlinear optical effect called SHG, also commonly called frequency doubling. This phenomenon requires intense laser light passing through a highly polarizable material with a noncentrosymmetric molecular organization—most typically an inorganic crystal. The second-harmonic light emerging from the material is at precisely half the wavelength of the light entering the material. Thus, the SHG process within the nonlinear optical material changes two near-infrared incident photons into one emerging visible photon at exactly twice the energy (and half the wavelength). As opposed to two-photon-excited fluorescence (TPEF), in which some of the incoming energy is lost during relaxation of the excited state, SHG does not involve an excited state, is energy conserving and

preserves the coherence of the laser light. Frequency-doubling crystals are commonly used to produce visible laser light from near-infrared lasers or UV light from visible lasers. **Box 1** provides a simplified summary of key equations underlying the theory of SHG.

Biological materials can be highly polarizable and often assemble into large, ordered noncentrosymmetric structures. Indeed, it has been known for 20 years that collagen can produce SHG signals[1] and for 15 years that biological membranes might be good general scaffolds for noncentrosymmetric arrays of SHG-active molecules[2,3]. However, it is only in the past few years that it has been shown that high-resolution SHG images can be obtained with instrumentation similar to that used for TPEF microscopy[4–11]. Like that of two-photon absorption, the amplitude of SHG is proportional to the square of the incident light intensity. Therefore, SHIM has the same intrinsic optical sectioning characteristic as TPEF microscopy. Thus, a new three-dimensional microscope contrast mechanism that does not require excitation of fluorescent molecules has been made available to the biological community.

The properties of SHG offer several advantages for live cell or tissue imaging. Because SHG does not involve excitation of molecules, it should not suffer, in principle, from phototoxicity effects or photobleaching, both of which limit the usefulness of fluorescence microscopy, including two-photon fluorescence microscopy, for the imaging of living specimens. (There can be collateral damage, however, if the incident laser light also produces two-photon excitation of chromophores in the specimen.) Another advantage is that many intrinsic structures produce strong SHG, so labeling with exogenous molecular probes is not required. On the other hand, electrochromic membrane dyes can be used to produce SHG that is highly sensitive to membrane potential. This may allow new optical approaches to be developed for mapping electrical activity in complex neuronal systems. Excitation uses near-infrared wavelengths, allowing excellent depth penetration, and thus this method is well suited for studying thick tissue samples.

Information about the molecular organization of chromophores, including dyes and structural proteins, can be extracted from SHG imaging data in several ways. SHG signals have well-defined polarizations, and thus SHG polarization anisotropy can be used to determine the absolute orientation and degree of organization of proteins in tissues. In addition, TPEF images can be collected in a separate data channel simultaneously with SHG. Correlation between the SHG and TPEF images provides the basis not only for molecular identification of the SHG source but also for probing radial and lateral symmetry within structures of interest. These special characteristics of SHIM as well as their current limitations are reviewed in this article.

Center for Biomedical Imaging Technology, Department of Physiology, University of Connecticut Health Center, Farmington, Connecticut 06030, USA. Correspondence should be addressed to L.M.L. (les@volt.uchc.edu).

Box 1 Theoretical background and fundamental equations

The nonlinear polarization for a material is defined by:

$$P = \chi^{(1)} \otimes E + \chi^{(2)} \otimes E \otimes E + \chi^{(3)} \otimes E \otimes E \otimes E + \dots \quad (1)$$

where P represents the induced polarization vector, E represents the vector electric field, $\chi^{(i)}$ is the ith-order nonlinear susceptibility tensor and $\otimes$ represents a combined tensor product and integral over frequencies. The $\chi^{(i)}$ corresponds to optical effects as follows:

- 1st-order process: absorption and reflection
- 2nd-order process: SHG, sum and difference frequency generation, hyper-Rayleigh
- 3rd-order process: multiphoton absorption, third harmonic generation, coherent anti-Stokes Raman scattering

The second nonlinear susceptibility is a bulk property and related to the molecular hyperpolarizability, β, by:

$$\chi^{(2)} = N_s < \beta > \quad (2)$$

where N_s is the density of molecules and the brackets denote an orientational average, which shows the need for an environment lacking a center of symmetry.

The second-harmonic intensities in such media will scale as follows:

$$SHG_{sig} \propto p^2 \tau (\chi^{(2)})^2 \quad (3)$$

where p and τ are the laser pulse energy and pulse width, respectively.

The magnitude of the SHG intensity can be strongly enhanced when the energy of the SHG signal ($2\hbar\omega$) is in resonance with an electronic absorption band ($\hbar\omega_{ge}$). Within the two-level system model, the first hyperpolarizability, β, and thus SHG efficiency is given by

$$\beta \approx \frac{3e^2}{2\hbar^3} \frac{\omega_{ge} f_{ge} \Delta\mu_{ge}}{[\omega_{ge}^2 - \omega^2][\omega_{ge}^2 - 4\omega^2]} \quad (4)$$

where e is electron charge and ω_{ge}, f_{ge} and $\Delta\mu_{ge}$ are the energy difference, oscillator strength (that is, integral of the absorption spectrum) and change in dipole moment between the ground and excited states, respectively. Because of the denominator in this equation, resonance-enhanced SHG has a dependence on the wavelength of the incident light similar to the two-photon excitation spectrum.

Because SHG is a coherent process, most of the signal wave propagates with the laser. The exact ratio of the forward to backward signal is dependent upon the sample characteristics. For thin samples, such as tissue culture cells, essentially the entire signal is directed forward. At higher sample turbidity, some of the SHG is scattered backward. The use of an upright microscope has some advantages for SHG imaging over that of an inverted geometry. The optical path is simpler for *trans* collection and this geometry also makes it more straightforward to implement the additional external optics required for polarization anisotropy measurements (described below). Commercial titanium sapphire femtosecond lasers are ideal for SHG (and TPEF) because of the high repetition rate (80 MHz) and high peak powers (and low pulse energies) and the broad tunability throughout the near infrared (700–1,000 nm). Because SHG intensities are typically smaller than those of TPEF, it is important to optimize the collection and detection efficiency for both signal isolation and detection electronics.

SHG imaging can also determine molecular symmetries by use of polarization analysis. SHG polarization anisotropy measurements are made with a Glan Laser Polarizer through which the data is obtained by maintaining the same input laser polarization and obtaining images with the analyzing polarizer oriented both parallel and perpendicular to the laser polarization. In addition, radial and lateral symmetries are probed by rotating the plane of polarization of the laser with half ($\lambda/2$) and quarter ($\lambda/4$) wave plates.

History and instrumentation

The first reports of the integration of SHG and microscopy appear to have been by Hellwarth and Christensen[12] in 1974 and Sheppard *et al.*[13] in 1977. To the best of our knowledge, the first biological SHG imaging experiments were done by Freund and colleagues in 1986 (ref. 1). The researchers used SHG to study the orientation of collagen fibers in rat tail tendon at ~50-μm resolution and showed that the collagen fibers formed highly dipolar structures at this scale. Initial reports by one of us (L.M.L.) and Lewis examined the second-harmonic response of styryl dyes in electric fields[14] and showed the possibility of imaging live cells by SHG[15]. In all this earlier work, stage scanning with a picosecond laser source focused through the microscope was used and frame rates of minutes to hours were required. To speed up the process, we modified a laser-scanning two-photon microscope to obtain SHG images with pixel density similar to that obtained with a standard confocal microscope with similar acquisition rates[4]. The enabling technologies that contributed to this advance were improved dye development, commercially available femtosecond titanium lasers and the use of single-photon counting for data acquisition. The last technology is required, especially for imaging dye-stained cells, because the SHG signal power per incident photon is much smaller than that for TPEF[16].

Endogenous imaging of structural protein arrays

Recently, it has been observed that very large SHG signals are directly obtainable from several structural protein arrays in tissues, without the addition of fluorescent dyes[6–11,17–22]. Our group[6,17,20,21] has examined structural proteins, including collagen, actomyosin complexes and tubulin, from several animal sources, among them mouse, tetra fish and *Caenorhabditis elegans*. Historically, these protein structures have been studied with other imaging modalities, including electron microscopy and polarization microscopy[23], and they are known to form arrays that are highly ordered and birefringent. The ability to image completely off resonance has the great benefit of the virtual elimination of photobleaching and phototoxicity, especially at longer wavelengths ($\lambda > 850$ nm). In addition, more detailed molecular information is readily elucidated than is possible through the use of fluorescent labels, even when dyes are conjugated to proteins. This is because dyes only infer details of protein assembly and motion, whereas SHG directly visualizes the submicrometer- and micrometer-scale assemblies.

One focus of our work—whose long-term goal is the study and diagnosis of muscle-related diseases—has been to investigate the use of SHG in studying the assembly of actomyosin complexes. It is important to determine the possible depth of penetration into muscle
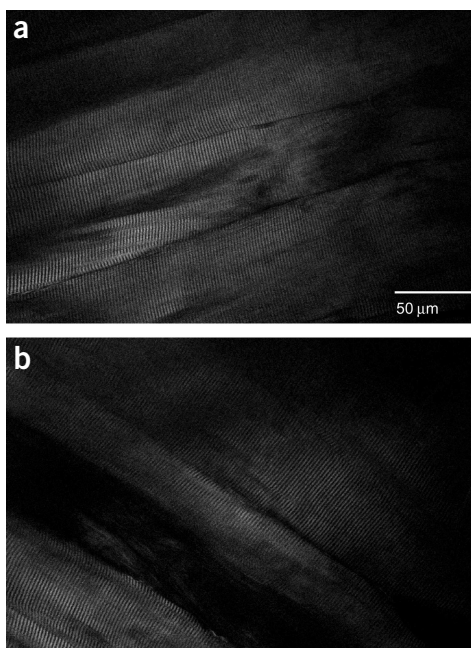
Figure 1 Endogenous SHG images of native mouse leg. (**a,b**) Within a 550-μm-thick tissue stack, images obtained from depths of ~200 μm (**a**) and 300 μm (**b**), respectively. The sarcomere repeat patterns are observed in both slices.

Figure 2 Endogenous SHG imaging of a living adult *C. elegans* nematode, showing two distinct axial slices. (**a**) The sarcomeres in the body wall muscles are seen at the edges of the animal, as well as in a portion of the chewing mechanism. (**b**) An optical section further into the same animal, where only the chewing mechanism is observed with substantial SHG intensity.

tissue as well as the molecular source of the SHG contrast. We address the first issue in **Figure 1**, which shows two slices of an explanted mouse leg muscle from regions approximately 200 and 300 μm deep from within a stack of tissue 550 μm thick. Despite the turbidity of muscle, these images display, with high contrast, the sarcomere repeat pattern that is characteristic of striated muscle. Indeed, only a fourfold loss of intensity was observed through the range of the entire stack. It should be noted that in all our work, we use the forward-detected geometry. In the present case, epidetection would have resulted in decreased signal intensity because less second harmonic is produced by backscattering, and the resulting lower-wavelength SHG light would undergo greater scattering losses as well. Nonetheless, the epidetection geometry may be the only viable method for imaging entire organs or entire, intact animals.

Although the SHG contrast of the sarcomeres resembles that seen by polarization microscopy, we have previously shown that the contrast is not identical. This is because the contrast in a polarization microscope arises from linear birefringence in the sample, whereas that of SHG arises from a quadratic process. The squared dependence on the protein concentration can then give rise to different features in the image. We see SHG as a more powerful imaging modality than polarization microscopy because of SHG's intrinsic sectioning and because polarization microscopy does not readily yield quantitative molecular level properties. In contrast, using the appropriate combinations of laser polarization and signal polarizations, all the relevant matrix elements of $\chi^{(2)}$ that give rise to the SHG signals can be determined, and thus yield the absolute orientation of fibrous structures and the degree of organization of the molecular dipoles. For example, using SHG polarization anisotropy, in which the laser polarization is kept fixed and the SHG signal is analyzed by a polarizer, we have observed that the collagen fibers in a tetra fish scale are highly anisotropic[6]. We determined the anisotropy parameter r using the expression for electric dipole distributions

$$r = \frac{I_{\mathrm{par}} - I_{\mathrm{perp}}}{I_{\mathrm{par}} + 2I_{\mathrm{perp}}}$$

where I_{par} and I_{perp} are the intensities of the signals whose polarizations are parallel and perpendicular, respectively, to the polarization of the incident laser. The limiting values of $r = 0$ and 1 correspond to the completely isotropic and aligned cases, respectively. We found an anisotropy parameter of $r = 0.7$, indicating that the dipoles in the collagen fibers form well-aligned structures. This type of data will be critical in the use of SHG in probing diseased states and differentiating between normal and abnormal tissue. For example, we are currently examining such differences in the micrometer-scale morphology of collagen fibers in the diseases osteogenesis imperfecta and tight skin through SHG imaging (P.J.C., unpublished data). One aspect to be determined in this work is the orientation of the molecular dipole relative to the long axis of the fibers. The SHG anisotropy approach of interrogating protein organization cannot achieve this directly by fluorescence anisotropy of dye-conjugated proteins because the loosely attached dye can rotate and 'wash out' some of the encoded structural information content.

We have also been similarly examining the molecular source of SHG in actomyosin complexes. In this work, we have largely used *C. elegans*, as these animals are optically clear and easy to manipulate genetically. Two frames of a three-dimensional stack of a live *C. elegans* nematode show the body wall muscles (**Fig. 2a**) and the chewing mechanism (**Fig. 2b**). To compare the SHG and fluorescence contrast, we raised *C. elegans* with green fluorescent protein (GFP)-labeled myosin and with myosin mutations, and showed that the SHG arises from the thick filaments. In particular, the data were consistent with the myosin heavy chain B isoform being the dominant source of SHG, with little contribution from either myosin heavy chain A or actin filaments. This example shows how the combination of simultaneous SHG and TPEF
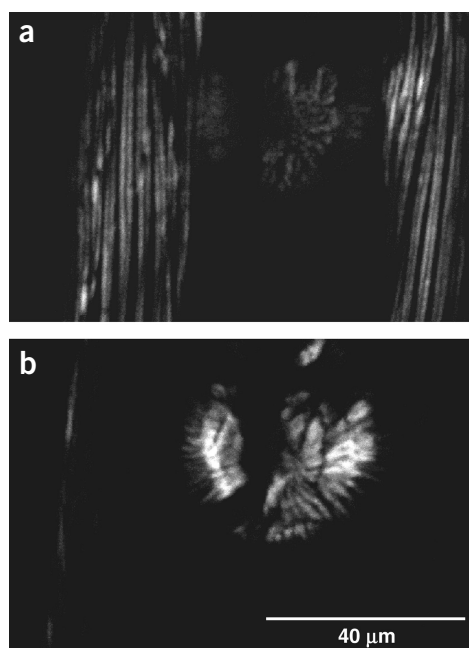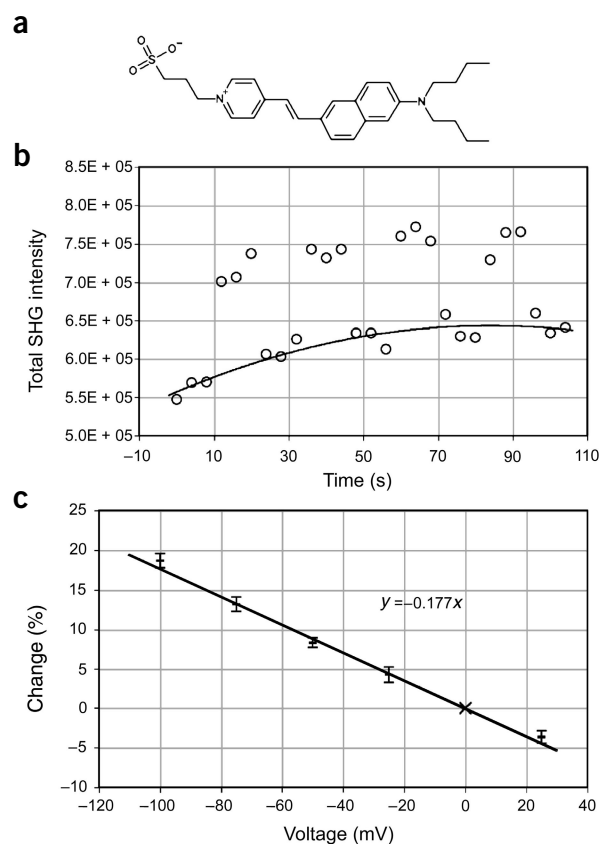
a

b

c

Figure 3 Membrane potential sensitivity of SHG from di-4-ANEPPS on a voltage-clamped N1E-115 neuroblastoma cell. (**a**) Structure of di-4-ANEPPS. (**b**) The results from a single experiment in which the cell is cycled between 0 mV and −100 mV every three image frames. Each point represents the integral of SHG intensity around the cell periphery. The dye is introduced shortly before the start of the image sequence and a small upward drift is seen as dye translocates from the bathing solution to the cell membrane. The incident laser is at 850 nm and SHG is detected at 425 nm. (**c**) The mean change in SHG as a function of membrane potential, with 0 mV as the reference. (Adapted from Millard et al.[29], by permission of the Optical Society of America.)

can be used to provide detailed structural data not possible by either alone. As our understanding of SHG in tissues expands, however, it will not always be necessary to use this combination imaging approach.

Although SHG is technologically much more complex, we see it as being a viable alternative to normal histologic analysis, as samples can be imaged in their natural state without fixation, labeling (and consequent photobleaching) and sectioning. Furthermore, SHG provides more complete structural information than polarization microscopy, as all the matrix elements of the second-order susceptibility that give rise to the contrast can be determined through the appropriate combinations of excitation and analyzer polarizations. We further expect that SHG will have a substantial impact on *in vivo* studies in various fields of biology and medicine, including tissue organization, wound healing, myofilament assembly, muscle development and disease, aging, and the division cycle of normal and cancerous cells *in situ*. The determination of the fundamental properties of the SHG contrast in simple model systems is the first, critical step in making the technique broadly useful.

Already, we and other researchers have begun to extend these methods to the analysis of fibrillar species in connective tissue and studies of

skin and muscle and brain pathology. For example, Jain and coworkers[24] have recently used SHG imaging to compare collagen content in tumors, identifying primarily type 1 collagen as the SHG source. Cox et al.[22] found that SHG can discriminate between type I and type III collagen in several tissue specimens. Similarly, Tromberg and colleagues[8] used SHG to probe the assembly of collagen in explanted rabbit corneas, to explore if SHG could be used as a nondestructive ophthalmological imaging tool. In other work, Webb and coworkers[10] showed that the polarity of microtubules is uniform in native brain and suggested that SHG could perhaps be used not only to probe neuronal polarity development, but also to investigate Alzheimer disease. SHG imaging enabled researchers in these studies to visualize the structural protein arrays directly (and quantitatively), rather than indirectly as with fluorescently tagged proteins or antibodies. As our understanding of the SHG process continues to expand, this may well become a useful tool complementary to ultra-resolution structural techniques such as electron microscopy or X-ray diffraction, which will provide a complete picture of tissue assembly.

SHIM of electrochromic membrane dyes
A consequence of equation (4) (**Box 1**) for resonance-enhanced SHG is that β depends on a large difference in the ground- and excited-state electron distribution (that is, a large $\mu_e - \mu_g$). This is also a key requirement for electrochromism—the sensitivity of the dye linear spectra to electric field. Our laboratory[25] has designed and synthesized a large number of electrochromic styryl dyes as fluorescent probes of membrane potential, and this led us to initially explore, in a fruitful collaboration with the laboratory of A. Lewis, the possibility that the dyes may produce large SHG signals[26]. In subsequent studies, we have used specially synthesized chiral dyes to boost the SHG signal[4,15,20,27]. It should be noted, however, that because population of the dye-excited state is a byproduct (via two-photon absorption) of resonance-enhanced SHG, some collateral photobleaching and phototoxicity may occur. We found that a strong SHG signal with achiral dyes is possible only if the dyes stain just one leaflet of the membrane bilayer—usually the outer leaflet because the dyes are applied from the external bath; if the dye equilibrates across the membrane, the requirement for a noncentrosymmetric distribution is violated and the SHG signal is abolished.

Using this class of dyes, SHIM has also been investigated in the laboratory of Mertz[5,28]. In addition to a thorough theoretical analysis of SHG cross-sections and polarization effects, they have shown that for aggregated lipid vesicles, regions where two membranes are in close apposition show no SHG, even though TPEF from these regions is strong; again, the close (less than the wavelength of the SHG signal) apposition of two stained membranes produces a symmetric distribution of dyes that does not allow SHG. Thus, TPEF and SHIM even from the same labeling dye can produce usefully different information, because the fluorescence signal and the second-harmonic signal arise from fundamentally different physics. In dual labeling experiments, complementary information is to be anticipated, as the SHG dyes can provide information about local structural organization, whereas fluorescent labels can provide information about molecular distributions.

The relationship between SHG and electrochromism shown in equation (4) (**Box 1**) also prompted us to ask whether SHG from membranes stained with our dyes could be sensitive to membrane potential. In our initial experiments, SHG from a dye-stained lipid bilayer was highly sensitive to membrane potential[14]. Experiments on live cells have confirmed this effect[4,15,29]. The sensitivity to membrane potential was most precisely revealed in recent voltage-clamp studies of neuroblastoma cells stained with one of our standard voltage-sensitive dyes, di-4-ANEPPS, in which the voltage was cycled from 0 to −100 mV every three frames[29] (**Fig. 3**). The SHG of di-4-ANEPPS was

linearly dependent on membrane potential, showing a relative change of 18% per 100 mV with a laser wavelength of 850 nm. The Mertz laboratory found similar sensitivities in a study of lipid vesicles placed in external uniform electric fields, and this group has also provided a detailed theory for the modulation of SHG by electric fields[30]. We have found that increasing the wavelength to 950 nm results in sensitivities of 40% per 100 mV (L.M.L., unpublished data). Such sensitivities are fourfold greater than can be achieved with the best fluorescence recordings of electrical activity with voltage-sensitive dyes.

Even so, a major challenge for the practical application of SHIM to the recording of electrical activity in neuronal systems is the SHG signal size. Although we have made great strides in reducing the acquisition time required to accumulate enough signal from many minutes for a 100×100 pixel image in the early experiments to just one second for a 512×512 pixel image in our current SHIM apparatus, this is still at least two orders of magnitude too slow to image action potentials. One approach is to limit the number of spatial points sampled in the laser scanning microscope, most commonly by scanning just single lines, so that data can be acquired more rapidly; of course, this will limit the ability to map electrical activity in a morphologically complex neuronal preparation. Another approach is to develop improved dyes with greater electrochromism and hyperpolarizabilities. A radically different strategy for dye development that has shown some preliminary promise[27,31,32] is to attach available electrochromic chromophores, such as aminonaphthyl derivatives (ANEPs), to silver or gold nanoparticles; the metal particles locally focus the laser electromagnetic field via a plasmon resonance effect, thereby enhancing SHG signals from neighboring dye molecules. We are working to develop easily deployable metal-dye conjugates to fully exploit this idea.

Conclusions

The promise of SHIM as a new tool for dynamic imaging of biological structure and function is now apparent. Nondestructive imaging of several endogenous proteins has been demonstrated and more examples are likely to be discovered. Detailed structural information as well as indications of pathology can be obtained from these images. Although the largest signals can be obtained in transmission configurations, it has also been shown that collagen can be imaged in a backscattering geometry. This will further extend the applicability of SHIM to studies of tissues in intact animals where transmitted light cannot be collected. For imaging membrane potential, the high sensitivity of the SHG signal promises to expand the application of optical recording of electrical activity in neuronal systems to the mapping of more complex preparations than had been previously possible. However, better dyes and improved optics will be needed to permit routine detection of action potentials by SHG. The simplicity of the modifications required to enable SHG detection in a multiphoton laser scanning microscope lead us to anticipate that this feature will shortly be offered by all the commercial manufacturers of these instruments. This will, of course, assure the dissemination of this exciting technology and prompt the discovery of new applications for both the basic research laboratory and the clinic.

COMPETING INTERESTS STATEMENT
The authors declare that they have no competing financial interests.

1. Freund, I., Deutsch, M. & Sprecher, A. Connective tissue polarity. Optical second harmonic microscopy, crossed-beam summation, and small-angle scattering in rat tail tendon. *Biophys. J.* **50**, 693–712 (1986).
2. Huang, Y.A., Lewis, A. & Loew, L.M. Nonlinear optical properties of potential sensitive styryl dyes. *Biophys. J.* **53**, 665–670 (1988).
3. Rasing, T., Huang, J., Lewis, A., Stehlin, T. & Shen, Y.R. *In situ* determination of induced dipole moments of pure and membrane-bound retinal chromophores. *Phys. Rev. A* **40**, 1684–1687 (1989).
4. Campagnola, P.J., Wei, M.–d., Lewis, A. & Loew, L.M. High-resolution optical imaging of live cells by second harmonic generation. *Biophys. J.* **77**, 3341–3349 (1999).
5. Moreaux, L., Sandre, O., Blanchard–Desce, M. & Mertz, J. Membrane imaging by simultaneous second harmonic generation and two-photo microscopy. *Optics Lett.* **25**, 320–322 (2000).
6. Campagnola, P.J. *et al.* Three-dimensional high-resolution second harmonic generation imaging of endogenous structural proteins in biological tissues. *Biophys. J.* **82**, 493–508 (2002).
7. Zoumi, A., Yeh, A. & Tromberg, B.J. Imaging cells and extracellular matrix *in vivo* by using second harmonic generation and two-photon excited fluorescence. *Proc. Natl. Acad. Sci. USA* **99**, 11014–11019 (2002).
8. Yeh, A.T., Nassif, N., Zoumi, A. & Tromberg, B.J. Selective corneal imaging using combined second harmonic generation and two-photon excited fluorescence. *Optics Lett.* **27**, 2082–2084 (2002).
9. Zipfel, W.R. *et al.* Live tissue intrinsic emission microscopy using multiphoton–excited native fluorescence and second harmonic generation. *Proc. Natl. Acad. Sci. USA* **100**, 7075–7080 (2003).
10. Dombeck, D.A. *et al.* Uniform polarity microtubule assemblies imaged in native brain tissue by second harmonic generation microscopy. *Proc. Natl. Acad. Sci. USA* **100**, 7081–7086 (2003).
11. Brown, E. *et al.* Dynamic imaging of collagen and its modulation in tumors *in vivo* using second harmonic generation. *Nat. Med.* **9**, 796–800 (2003).
12. Hellwarth, R. & Christensen, P. Nonlinear optical microscopic examination of structure in polycrystalline ZnSe. *Optics Comm.* **12**, 318–322 (1974).
13. Sheppard, C.J.R., Kompfner, R., Gannaway, J. & Walsh, D. Scanning harmonic optical microscope. *IEEE J. Quantum Electron.* **13E**, 100D (1977).
14. Bouevitch, O., Lewis, A., Pinevsky, I., Wuskell, J.P. & Loew, L.M. Probing membrane potential with non-linear optics. *Biophys. J.* **65**, 672–679 (1993).
15. Ben-Oren, I., Peleg, G., Lewis, A., Minke, B. & Loew, L.M. Infrared nonlinear optical measurements of membrane potential in photoreceptor cells. *Biophys. J.* **71**, 1616–1620 (1996).
16. Moreaux, L., Sandre, O. & Mertz, J. Membrane imaging by second harmonic generation microscopy. *J. Opt. Soc. Am. B* **17**, 1685–1694 (2000).
17. Mohler, W., Millard, A.C. & Campagnola, P.J. Second harmonic generation imaging of endogenous structural proteins. *Methods* **29**, 97–109 (2003).
18. Stoller, P., Reiser, K.M., Celliers, P.M. & Rubenchik, A.M. Polarization-modulated second harmonic generation in collagen. *Biophys. J.* **82**, 3330–3342 (2002).
19. Stoller, P., Kim, B.M., Rubenchik, A.M., Reiser, K.M. & Da Silva, L.B. Polarization-dependent optical second harmonic imaging of a rat-tail tendon. *J. Biomed. Opt.* **7**, 205–214 (2002).
20. Campagnola, P.J., Clark, H.A., Mohler, W.A., Lewis, A. & Loew, L.M. Second harmonic imaging microscopy of living cells. *J. Biomed. Opt.* **6**, 277–286 (2001).
21. Millard, A.C., Campagnola, P.J., Mohler, W., Lewis, A. & Loew, L.M. Second harmonic imaging microscopy. *Methods Enzymol.* **361**, 47–69 (2003).
22. Cox, G. *et al.* 3-dimensional imaging of collagen using second harmonic generation. *J. Struct. Biol.* **141**, 53–62 (2003).
23. Inoue, S. *Video Microscopy* (Plenum Press, New York, 1986).
24. Brown, E. *et al.* Dynamic imaging of collagen and its modulation in tumors *in vivo* using second harmonic generation. *Nat. Med.* **9**, 796–800 (2003).
25. Loew, L.M. in *Fluorescent and Luminescent Probes for Biological Activity* (ed. Mason, W.T.) 210–221 (Academic Press, London, 1999).
26. Huang, J.Y., Lewis, A. & Loew, L.M. Non-linear optical properties of potential sensitive styryl dyes. *Biophys. J.* **53**, 665–670 (1988).
27. Clark, H.A., Campagnola, P.J., Wuskell, J.P., Lewis, A. & Loew, L.M. Second harmonic generation properties of fluorescent polymer encapsulated gold nanoparticles. *J. Am. Chem. Soc.* **122**, 10234–10235 (2000).
28. Moreaux, L., Sandre, O., Charpak, S., Blanchard–Desce, M. & Mertz, J. Coherent scattering in multi-harmonic light microscopy. *Biophys. J.* **80**, 1568–1574 (2001).
29. Millard, A.C., Jin, L., Lewis, A. & Loew, L.M. Direct measurement of the voltage sensitivity of second harmonic generation from a membrane dye in patch-clamped cells. *Optics Lett.* **28**, 1221–1223 (2003).
30. Moreaux, L., Pons, T., Dambrin, V., Blanchard–Desce, M. & Mertz, J. Electro–optic response of second harmonic generation membrane potential sensors. *Optics Lett.* **28**, 625–627 (2003).
31. Peleg, G. *et al.* Gigantic optical non-linearities from nanoparticle enhanced molecular probes with potential for selectively imaging the structure and physiology of nanometric regions in cellular systems. *Bioimaging* **4**, 215–224 (1996).
32. Peleg, G., Lewis, A., Linial, M. & Loew, L.M. Nonlinear optical measurement of membrane potential around single molecules at selected cellular sites. *Proc. Natl. Acad. Sci. USA* **96**, 6700–6704 (1999).